Published in final edited form as:
Pain. 2008 June ; 136(3): 407–418.

Acupuncture Modulates Resting State Connectivity in Default and Sensorimotor Brain Networks

Rupali P. Dhond[1,2], **Calvin Yeh**[1], **Kyungmo Park**[1,3], **Norman Kettner**[2], and **Vitaly Napadow**[1,2]

1*MGH/MIT/HMS Martinos Center for Biomedical Imaging, Charlestown, MA*

2*Department of Radiology, Logan College of Chiropractic, Chesterfield, MO*

3*Department of Biomedical Engineering, Kyunghee University, Yongin, Korea*

Abstract

Previous studies have defined low-frequency, spatially consistent networks in resting fMRI data which may reflect functional connectivity. We sought to explore how a complex somatosensory stimulation, acupuncture, influences intrinsic connectivity in two of these networks: the default mode network (DMN) and sensorimotor network (SMN). We analyzed resting fMRI data taken before and after verum and sham acupuncture. Electrocardiography data was used to infer autonomic modulation through measures of heart rate variability (HRV). Probabilistic independent component analysis was used to separate resting fMRI data into DMN and SMN components. Following verum, but not sham, acupuncture there was increased DMN connectivity with pain (anterior cingulate cortex (ACC), periaqueductal gray), affective (amygdala, ACC), and memory (hippocampal formation, middle temporal gyrus) related brain regions. Furthermore, increased DMN connectivity with the hippocampal formation, a region known to support memory and interconnected with autonomic brain regions, was negatively correlated with acupuncture-induced increase in a sympathetic related HRV metric (LFu), and positively correlated with a parasympathetic related metric (HFu). Following verum, but not sham, acupuncture there was also increased SMN connectivity with pain related brain regions (ACC, cerebellum). We attribute differences between verum and sham acupuncture to more varied and stronger sensations evoked by verum acupuncture. Our results demonstrate for the first time that acupuncture can enhance the post-stimulation spatial extent of resting brain networks to include anti-nociceptive, memory, and affective brain regions. This modulation and sympathovagal response may relate to acupuncture analgesia and other potential therapeutic effects.

INTRODUCTION

Acupuncture is an ancient Eastern healing modality which may have therapeutic effects in the treatment of chronic pain [8,50] and other illnesses. A review of the literature suggests that acupuncture influences a diverse set of bodily organs and functions including brain processing [25,26] and autonomic nervous system (ANS) activity [1,44].

Address Correspondence To: Vitaly Napadow, PhD Assistant Professor Martinos Center for Biomedical Imaging Massachusetts General Hospital Boston, Massachusetts vitaly@nmr.mgh.harvard.edu.

It has long been known that the analgesic effects of acupuncture may actually peak long after cessation of active needle stimulation [58]. Furthermore, clinical acupuncture typically involves an active needle manipulation phase followed by a longer period of rest. Thus, although many fMRI studies have investigated brain response to acute needle *stimulation*, none have evaluated acupuncture effects on functional connectivity that may extend beyond the active needle stimulation phase, i.e. *sustained* acupuncture effects.

To investigate the sustained effects of acupuncture into post-stimulus rest, we evaluated functional connectivity changes in "resting state networks," RSNs. Previous fMRI studies have found that in a task-free state (i.e. rest), multiple distributed brain areas demonstrate temporal correlation or intrinsic "functional connectivity" in low frequency ranges [11,22,32,46]. For example, studies have found correlation in resting fMRI signal from sensorimotor cortices of opposite hemispheres [11]. This RSN has been referred to as the sensorimotor network, or SMN [6]. Resting connectivity has also been described in the default mode network (DMN) [14,30,35], which involves brain regions putatively engaged in self-referential cognition that are "deactivated" during a variety of externally focused task conditions [for review see 38]. Pain is known to interact with the DMN. Both acute pain [59] and acupuncture [54] are known to induce deactivation in DMN regions, while chronic pain may be associated with less pronounced DMN deactivation in response to a visual attention task [2]. Furthermore, perception of somatosensory stimuli near sensory threshold is facilitated by decreased DMN activity in a brief pre-event resting period [12].

Our study aimed to resolve the change in resting functional connectivity following a complex somatosensory stimulation, acupuncture, using probabilistic Independent Component Analysis (pICA), which can separate fMRI data into independent RSNs, including the DMN and SMN [6]. Furthermore, recent reports have suggested that ANS response to acupuncture (measured by heart rate variability, HRV, [49]) may be linked to clinical response for different chronic pain populations [60]. As variable peripheral ANS response to acupuncture may influence post-stimulation brain activity, we also sought to explore the relationship between acupuncture induced ANS outflow to the heart as estimated by HRV and acupuncture induced changes in RSN connectivity. To our knowledge, this study constitutes the first investigation of the sustained effects of somatosensory stimulation on resting state connectivity.

METHODS

Subjects and Experimental Design

Data was collected for 15 healthy, right handed [57] adults (8 female), 21−33 years of age. Subjects were recruited via fliers/newsletters adhering to MGH guidelines for distribution at neighboring academic institutions and hospitals. Subjects were screened to assure their safety and compatibility with MRI recording.

The present study involved verum manual acupuncture (ACUP) and sham acupuncture (SHAM). Both ACUP and SHAM consisted of a total of 150 seconds of active stimulation in a blocked design paradigm. A 5.5 minute rest run was completed before, and after, each active stimulation run (Figure 1). During rest runs, subjects were asked to lie quietly and fixate on a centrally presented "+". Past studies have demonstrated robust RSN activity for both eyes closed, and eyes open, with and without fixation [31]. Fixation was chosen in order to minimize drowsiness and the potential for sleep.

The order of ACUP and SHAM runs was randomized across subjects to mitigate order effects. These two runs (and their respective rest runs) were separated by structural scans which lasted at least 15 minutes total in order to maximize washout of acute stimulation effects within the

scan session. Data from the rest run immediately following acupuncture were compared to data from the rest run immediately preceding stimulation (i.e. after – before acupuncture).

All acupuncture was performed by the same licensed (and experienced) acupuncturist at left PC-6. This acupoint, which is on the volar aspect of the forearm, is 2 cun (~5cm) proximal to the transverse wrist crease, between the tendons of the palmaris longus and flexor carpi radialis muscles. For ACUP, acupuncture was performed by first inserting a non-magnetic (pure silver), 0.23mm diameter, 30mm long acupuncture needle (Asahi Industry, Inc., Kawaguchi, Japan) into PC-6 to a depth of approximately 1.5cm. During stimulation, the needle was manually twirled (~±180°) at 0.5 Hz.

For SHAM, needle insertion was first simulated by poking the skin over PC-6 with a 5.88 von Frey monofilament passed through a needle guide tube (similar to the one used for verum acupuncture). During the scan run, the acupuncturist performed non-insertive cutaneous stimulation over the acupoint (tapping at 0.5 Hz) using the same monofilament. Subjects were acupuncture-naive and were not informed of a sham acupuncture condition, only that there would be “different forms” of acupuncture during fMRI. Subjects lay supine in the scanner with their vision of distal body regions blocked by the MRI head coil, preventing them from viewing the intervention occurring at their periphery. The issue of appropriate controls in acupuncture research remains controversial [39]. Each type of control addresses different aspects of the acupuncture intervention. For example, non-insertive stimulation at the acupoint controls for the cutaneous somatosensory (and potentially cognitive) aspect of the intervention. Thus, any differences found between verum and sham acupuncture are most likely attributable to needle penetration and stimulation of deeper, subcutaneous mechanoreceptors and/or nociceptors. In contrast, insertive needling at a nonacupoint controls for the insertive nature, and potentially cognitive aspects, of the intervention. Thus, any differences between verum and sham might be more strongly attributed to acupoint-specificity, which has been posited by traditional East Asian medical theory. In this experiment, we chose to emphasize the stimulation of deep receptors as the active component of acupuncture and used a non-insertive sham acupuncture control, delivered over the same cutaneous location on the body. Our sham stimulation aimed to control for both superficial, cutaneous somatosensory effects over the acupoint, as well as the cognitive processing induced by subjects expecting “acupuncture” stimulation.

Imaging Data Collection and Analysis

FMRI Data were acquired using a 3T Siemens Tim Trio MRI System (Siemens Medical, Erlangen, Germany) equipped for echo planer imaging with a 12 channel head coil. During scanning, subjects remained in the supine position with their heads immobilized by cushioned supports. Subjects wore earplugs throughout the experiment to attenuate MRI gradient noise. Structural scans consisted of a T1-weighted anatomical (TR/TE = 2.73/3.19 ms, flip angle = 7°, FOV = 256×256 mm; slice thickness = 1.33 mm) and a multi-echo fieldmap scan (f.a.=55°, $TR/TE_1/TE_2$ = 500/3.38/5.84 ms). Blood oxygenation level-dependent (BOLD) functional imaging was performed using a gradient echo T2*-weighted pulse sequence (TR/TE=3000/30 ms, flip angle = 90°, FOV = 200 × 200 mm, 48 coronal slices, slice thickness = 3.0 mm with 0.6 mm interslice gap, matrix = 64 × 64, 110 time points for a total of 5.5minutes). Image collection was preceded by 5 dummy scans. Coronal slices were used to minimize susceptibility artifact (gradient distortion) in subcortical limbic regions [56].

Data analysis was performed using a combination of analysis packages including FSL (FMRIB's Software Library) and AFNI. Functional data were pre-processed to correct for magnetic field inhomogeneities caused by magnetic susceptibility differences in neighboring tissues within the head (FSL-FUGUE) and motion corrected to compensate for any head movements using a linear (affine) transformation procedure (FSL-FLIRT). Brain extraction

was performed on functional data using FSL-BET while skull stripping of structural data for alignment utilized Freesurfer Software [20,28]. Functional data were smoothed using a Gaussian kernel of FWHM 5 mm; and high-pass temporal filtering (f = 1/250 s) was also performed.

Independent component analysis (ICA) was performed on all rest runs using FSL-MELODIC [7]. The use of probabilistic Independent Component Analysis (pICA) to derive RSNs has been successfully performed in the past by several groups [6,34] in order to evaluate functional connectivity networks. The independent components (IC) maps are in the form of a Z-statistic for which activated/deactivated areas may be considered temporally coherent. While some groups have utilized seed-voxel approaches to investigate resting state functional connectivity, these methods require a priori selection of regions of interest which imposes a subjective element to data analysis. ICA also has the advantage of being able to better separate/remove low frequency components due to physiological noise which may more readily contaminate seed voxel analyses of functional connectivity [10].

In the present analysis, the number of output IC's was not restricted and subsequent component masking and selection procedures were similar to those applied in Greicius et al. (2007). Specifically, the ICA components were first screened for the presence of high frequencies (> 0.1Hz) by rejecting those components which had more than 25% of their total Fourier spectrum power in frequencies above 0.1Hz. Our investigation focused on acupuncture modulation of DMN and SMN activity, as regions within these networks have been found to respond in our block-design fMRI studies of acupuncture [54]. Templates of both the DMN and SMN were then used to select the “best-fit” components for each rest run in all subjects. Typically, the DMN includes the inferior parietal lobule (IPL) (~BA 40, 39), the posterior cingulate (~BA 30, 23, 31) and precuneus (~BA 7), areas of the inferior, medial and superior frontal gyri (~BA 8, 9, 10, 47), the hippocampal formation, and the lateral temporal cortex (~BA 21) [14]. The SMN includes bilateral primary and secondary somatosensory areas (SI and SII), primary motor cortex (MI), and the SMA [6,11]. The templates were RSN group maps (thresholded at $p<0.05$) from healthy adults which were provided by Beckmann [6], who also used pICA for their derivation (**see** Figure 2).

The best-fit component was selected by calculating the average z-score of voxels both inside and outside of the template then selecting the component for which the ratio of values inside/outside was the greatest. Subsequent group analysis was performed on the selected component maps using a mixed effects model (FSL-FEAT). It is important to note that these component maps contained whole-brain data and were un-masked, thereby preserving any significant connectivity that regions within the DMN and SMN may have with regions outside the classically defined borders outlined in the templates. Paired t-tests were performed to determine differences in spatial extent between resting state networks (DMN and SMN) before vs. after the acupuncture runs, thresholded at a corrected cluster significance level of $p=0.05$. Unpaired t-tests versus nil were performed to derive group maps for SMN and DMN connectivity both before and after acupuncture, also thresholded at a corrected cluster significance level of $p=0.05$. Anatomical localization was assisted by use of a brain atlas [47]. Cerebellar localization was aided by recent work in MRI-guided parcellation [48].

Cardiorespiratory Physiology Data Acquisition and Analysis

In order to infer cardiac sympathovagal modulation by acupuncture, subjects were outfitted with MRI-compatible chest ECG electrodes and a nasal cannula to measure end tidal CO_2. Electrocardiogram (ECG) and respiratory data were collected at 200Hz with a system specially designed to mitigate MRI-induced artifact in the ECG trace (InVivo Magnitude CV, Invivo Research Inc., Orlando, Florida), on a laptop acquisition system (Labview 7.0, DAQCard 6024E, National Instruments, Austin, Texas) for further analysis.

ECG data were processed with the WFDB (WaveForm DataBase) Software Package [33] and MATLAB 6.5 (The Mathworks, Inc. Natick, MA). Data were automatically annotated with careful manual correction in order to form an RR-interval time series. A power spectrum of this time series was then calculated using the maximum entropy (all-poles) method [33]. Low frequency (LF) and high frequency (HF) power were estimated by integrating within the 0.04 −0.15Hz and 0.15−0.50Hz frequency bands, respectively. These metrics were calculated in normalized units by dividing the LF and HF values by the total power minus that in the very low frequency range (0−0.04Hz), and termed LFu and HFu [49]. While some controversy in interpretation remains, LFu is more influenced by cardio-sympathetic activity, while HFu is influenced solely by cardiovagal activity [49]. The respiratory data were used to ensure that respiratory rate did not drop below 0.15Hz or rise above 0.40Hz, a requisite for subdividing the LF and HF power bands and attributing sympathetic and parasympathetic interpretation to LFu, and HFu. For correlation analysis, normalized individual response to ACUP and SHAM was calculated by subtracting the value in the pre-stimulation rest from the value during active stimulation. To investigate the relation between these metrics and imaging results (post-pre change in mean z-statistic within ROIs significant from the paired t-test above), Pearson correlation coefficients were calculated, significant at $p<0.05$.

Psychophysical Data Collection and Analysis

Following the ACUP and SHAM portions of the scan session, subjects rated the intensity of sensations they felt during the active stimulation run. Subjects were presented with a 10 point visual analog scale (VAS) and were asked to rate the intensity of sensations commonly associated with the experience of *deqi*[¥], and listed on the MGH Acupuncture Sensation Scale (MASS). Subjects also assessed anxiety/relaxation on a scale ranging from very anxious (5) to fully relaxed (−5). Additionally, subjects were asked to assess the extent of “spreading” that may have occurred for any of the listed sensations. A modified version of this procedure has been successfully used by our group in the past to assess psychophysical response in conjunction with neuroimaging [41,54]. In order to quantify the total amplitude of *deqi* experienced we used the *MASS-Index*, which is calculated by an exponentially decreasing weighted sum of all sensations [45]. This index attempts to balance breadth and depth of sensations as well as the number of different sensations chosen by the subject. The MASS index was compared between stimulation groups using a paired t-test, significant at $p<0.05$ (SPSS 10.0.7, Chicago, Illinois). Furthermore, frequency counts of specific sensations were compared between stimulation type with a Pearson Chi-squared test, significant at $p<0.05$. An omnibus test (Fisher's combined probability test) was used to test if the commonality of sensations elicited by ACUP differed from those elicited by SHAM.

To investigate the relation between the intensity of elicited sensations and imaging results (post-pre change in mean z-statistic within ROIs significant from the paired t-test above), Pearson correlation coefficients were calculated. Sensations included in this analysis were those reported by greater than 60% of subjects, as too many nil values would adversely skew the distribution. Results were deemed significant at $p<0.05$, Bonferroni corrected for multiple comparisons due to the large number of sensations tested (9).

Finally, in order to investigate the persistence of sensations into the rest run following active stimulation, we also asked subjects to rate the intensity of sensation during the rest run before and after verum and sham stimulation. For these data, sensation intensity difference between verum and sham acupuncture was contrast using a paired t-test, significant at $p<0.05$.

[¥] *Deqi* corresponds to a multitude of different pain-like and non-pain sensations experienced by a needled subject and is a correlate of effective treatment [63].

RESULTS

Results of RSN Analysis

Group maps of the best fitting independent components for the DMN and SMN demonstrated consistently robust spatial distribution relative to their respective templates, both before and after verum (Figure 2) and sham (data not shown) acupuncture. The best fitting component for the DMN demonstrated resting connectivity within the inferior parietal lobule, posterior cingulate, and medial areas of the inferior, middle and superior frontal gyri, as well as the precuneus. The best fitting component for the SMN involved bilateral primary somatosensory and motor cortices, secondary somatosensory cortex and the supplementary motor area (SMA).

When comparing DMN connectivity after ACUP with that before, there was increased connectivity of this network to a number of areas (Figure 3, Table 1) including the amygdala, hippocampal formation, periaqueductal gray (PAG), substantia nigra (SN), middle temporal gyrus (MTG, ~BA 21), supplementary motor area (SMA), and anterior cingulate (ACC, ~BA 24), posterior parietal (~BA 7), and primary visual (V1) cortices. There were no areas of decreased connectivity following ACUP. Conversely, after SHAM, the DMN demonstrated increased connectivity with only the temporo-occipital cortex (~BA 37/39) and decreased connectivity with areas of the middle (~BA 21) and inferior temporal (~BA 20) gyri (Figure 3, Table 1). This “decreased” connectivity resulted from a greater z-score before SHAM than after (2 rightmost columns, Table 1)

After ACUP, the SMN demonstrated increased connectivity with the anterior cingulate cortex (~BA 32/24), pre-SMA (~BA 8/6), and cerebellum (simplex, lateral hemispheric zone 1, VI *l*) (Figure 4, Table 1). Conversely, after SHAM, the SMN demonstrated decreased connectivity with the dorsolateral prefrontal cortex (~BA 8, greater before versus after, Figure 4, Table 1).

RSN Correlation with Acupuncture-induced ANS modulation

In order to explore the relationship between changes in brain functional connectivity and acupuncture-induced ANS modulation, we calculated the inter-subject Pearson correlation coefficient between the change in HRV metrics (LFu, HFu) during acupuncture minus the pre-stimulus rest and the change in z-statistic in ROIs taken from significant regions from the paired t-test above for both DMN and SMN. The metrics demonstrated consistent correlation with increasing hippocampal formation connectivity to the DMN following ACUP (LFu: $r = -0.73$, HFu: $r = 0.68$, $p<0.01$, Figure 5). This result suggests that increased parasympathetic and decreased sympathetic modulation during ACUP is associated with increased post-ACUP DMN connectivity with the hippocampal formation. In addition, the change in post-ACUP DMN connectivity with the MTG also demonstrated a negative correlation with LFu ($r = -0.70$, $p<0.01$). These data passed the Grubb's test for outliers ($p<0.05$). No other significant correlations were found for either ACUP or SHAM, though it should be remembered that correlations were tested only for regions significant in the fMRI group analysis (paired t-test). Thus, while regions such as the insula (particularly the right anterior insula) are associated with the central autonomic network and have demonstrated brain response correlated with HRV [19], the insula was not a region which demonstrated either increased or decreased connectivity to either the DMN or SMN following acupuncture and was not included in this analysis.

Results of Psychophysical Analysis

A statistical analysis found that MASS Index, a measure of *deqi* intensity, was greater for ACUP compared to SHAM stimulation (paired t-test, $p<0.01$). Furthermore, there was a greater intensity (paired t-test, $p<0.05$) of spreading for ACUP (3.6 ± 2.4) compared to SHAM (1.7 ± 1.5). Interestingly, SHAM was associated with greater relaxation (-1.2 ± 2.4, $\mu\pm\sigma$) compared to ACUP (0.2 ± 2.3, $\mu\pm\sigma$). There was no significant difference in the intensity of sharp pain

(ACUP: 3.7±2.7; SHAM: 4.9±2.6) or throbbing (ACUP: 3.9±1.9; SHAM: 2.6±2.4). An omnibus test (Fisher's combined probability test) found that ACUP and SHAM also differed in the commonality of sensations, $p(n=14) < 0.001$. Differences also existed in the prevalence of specific *deqi* sensations elicited (Figure 6). The prevalence of "aching" (ACUP: 86.7% of subjects, SHAM: 40.0%, $p<0.01$), "fullness" (ACUP: 46.7%, SHAM: 13.3%, $p<0.05$), and "dull pain" (ACUP: 93.3%, SHAM: 40.0%, $p<0.005$) was found to be greater for ACUP (uncorrected for multiple comparisons due to significant omnibus test). It should also be noted that while sharp pain was reported for both conditions, when debriefed, most subjects who reported sharp pain described this sensation as only transient, occurring typically at the start of a stimulation block.

We also wanted to explore the relationship between changes in brain functional connectivity and the intensity of sensations evoked by acupuncture. We calculated the inter-subject Pearson correlation coefficient between the intensity of acupuncture-evoked sensations and the change in z-statistic in ROIs taken from the paired t-test above for both DMN and SMN. We found a trend for increasing ACUP evoked "soreness" correlating with increasing SMN connectivity with pre-SMA ($r = 0.65$, $p=0.081$, Bonferroni corrected). This result is consistent with the hypothesis that changes in resting SMN connectivity, a network containing brain regions subserving the sensory-discriminative aspects of pain, are related to the sensations evoked by acupuncture stimulation. No significant correlations were found for DMN ROIs, nor for any ROIs from the sham acupuncture paired t-test.

For the rest runs following ACUP and SHAM, sensation intensity scores were collected for 11 subjects. Of these, four subjects reported feeling any sensation at some point during the rest run immediately following ACUP (0.9 ± 1.3, overall $\mu\pm\sigma$) and two following SHAM (0.4 ± 0.8). Ultimately, there was no significant difference between mean sensation intensity in the rest runs following ACUP versus those following SHAM ($p>0.1$).

DISCUSSION

Acupuncture has shown promise in treating chronic pain and other disorders [55]. Acupuncture analgesia for chronic pain is typically delayed from the needle stimulation phase and may result from modulation of brain processing and/or autonomic response sustained into the post-stimulation period. We used pICA to evaluate acupuncture modulation of functional connectivity within RSNs consistent with the DMN and SMN. Following ACUP, but not SHAM, there was increased DMN connectivity with limbic anti-nociceptive (ACC, PAG), affective (amygdala, ACC), and memory (hippocampal formation, MTG) related brain regions. Furthermore, increased DMN connectivity with the hippocampal formation, a region known to support memory and interconnected with autonomic motor nuclei, was anti-correlated with acupuncture-induced increase in a sympathetic related HRV metric (LFu), and correlated with a parasympathetic related HRV metric (HFu). In addition, following ACUP, there was greater connectivity between SMN and pain processing and motor planning brain regions (ACC, pre-SMA, and cerebellum), changes not seen following SHAM. These results demonstrate for the first time that a somatosensory stimulation can have sustained effects on brain resting state connectivity.

Changes in DMN functional connectivity following acupuncture

Previous studies have defined the DMN as a set of regions demonstrating increased hemodynamic activity at baseline relative to a variety of active (i.e. goal oriented) task conditions [38]. The precise function of the DMN is debated, but evidence suggests that it may support autobiographical memory and decreased externally focused attention [14]. Importantly, the DMN is mainly comprised of cortical "association areas" and thus has

extensive anatomical connections with not only primary sensory areas but also subcortical regions involved in pain processing, affect, and memory encoding/retrieval.

Our results found that ACUP enhanced resting DMN connectivity with the ACC, PAG, and SN - areas putatively involved in affective pain processing/evaluation, pain anticipation and endogenous anti-nociception. The dorsal subregion of the ACC (BA 24) is activated by acute painful stimuli [21]. This limbic area is also activated in endogenous anti-nociception [23], affective pain processing [27], and attention to painful stimuli [3]. Moreover, ACUP increased resting DMN connectivity with other anti-nociceptive regions such as the PAG. Animal studies of acupuncture suggest that opioidergic modulation of the PAG plays a critical role in acupuncture analgesia via inhibition of afferent pain signaling [40]. In addition, acupuncture related opioidergic modulation of the PAG also supports sympatho-inhibition [37,61]. It is likely that these functions are inter-related, as the sympathetic nervous system is known to up-regulate pain circuitry and vice versa [42]. The SN is the primary source of dopaminergic (DA) input to the striatum. The DA system projects diffusely to many brain regions, and the SN has been implicated in pain and non-pain somatosensory perception, especially when stimuli have high behavioral context [for review see 16]. We propose that increased DMN connectivity with brain areas involved in anti-nociception and sympatho-inhibition forms the basis of an integrated network for top-down regulation of acupuncture analgesia.

Other areas demonstrating increased connectivity with DMN following ACUP are most often implicated in memory encoding/retrieval (hippocampal formation) and affective memory (amygdala) but are also modulated during experimental pain [4,9,13,24]. Our previous block design fMRI studies demonstrated that acupuncture reduces activity within the amygdala and hippocampal formation [53], a potential region of the DMN [14,36]. Our data suggests that this reduction may be sustained minutes after acupuncture stimulation and manifest as increased connectivity between these regions and the DMN. Interestingly, it has been suggested that chronic pain leads to ‘pain memories’ which can persist long after the peripheral pain source has resolved, leading to centrally driven pain [29,43]. Non-pain somatosensory memories have also been noted [43]. We propose that acupuncture sensations, which combine dull pain and deep, unusual somato-sensations, can form somatosensory memories by binding the DMN with pain-related, affective and memory related regions. If this sustained connectivity can be coupled with brain processing in anti-nociceptive brain regions, over multiple treatment sessions, the linkage may help erode centrally driven chronic pain memories. While speculative, this hypothesis is supported by clinical acupuncture practice, which typically demands multiple, regularly spaced treatment sessions.

Increased DMN connectivity in the above regions was not found following another complex somatosensory intervention, SHAM. Our psychophysical data demonstrated that compared to SHAM, ACUP induced more intense and more varied *deqi* sensations which spread more extensively away from the acupoint site. These differences in psychophysics were consistent with our past studies [53] and other data comparing verum and non-insertive shams (e.g. placebo-needles), which may better mimic needle *insertion* than needle *manipulation* [62]. Furthermore, only a small number of subjects experienced mild *deqi* sensations during rest (following both ACUP and SHAM). Thus, our results are likely due to the sensations experienced *during* stimulation and not bottom-up somatosensory persistence for either ACUP or SHAM. It is possible that increased somatosensory saliency (greater *deqi*) for ACUP promotes connectivity of DMN with areas supporting sensory stimulus encoding seen in our data, such as the posterior parietal cortex and SMA. Interestingly, tasks of greater cognitive complexity [51] and pain intensity [59] have been shown to more readily deactivate DMN brain regions. Our results demonstrate that increased somatosensory saliency may also influence DMN connectivity in the resting state *minutes after* active stimulation.

We also sought to explore the relationship between acupuncture-induced autonomic modulation and subsequent change in RSN connectivity. Increased DMN connectivity with the hippocampal formation was anti-correlated with acupuncture-induced increase in sympathetic modulation, and correlated with parasympathetic modulation. Interestingly, the hippocampus has polysynaptic connectivity with autonomic brainstem nuclei [15], while vagal nerve stimulation enhances memory [17], an effect that may be supported by hippocampal activity. Our data contribute to these results by suggesting that when acupuncture induces a sympathovagal shift toward parasympathetic, the hippocampal formation has greater connectivity with the DMN, a brain network thought to subserve self-referential cognition and autobiographical memory [14]. While pain is known to modulate autonomic outflow [18], the response is typically increased sympathetic tone. However, increased hippocampal/DMN connectivity following acupuncture was associated decreased sympathetic and increased parasympathetic modulation, suggesting that acupuncture modulation of DMN connectivity may not result from classic pain-like aspects of this complex intervention. Interestingly, other groups have found that acupuncture-induced decrease of LF/HF ratio, relating a shift in sympathovagal balance toward greater parasympathetic modulation, may relate to acupuncture therapeutic effects on chronic pain [60]. Our correlative results connecting HRV metrics with enhanced DMN connectivity should to be replicated in a clinical population to investigate this possible connection with clinical efficacy.

Changes in SMN functional connectivity following acupuncture

Following ACUP, the SMN demonstrated increased connectivity with the ACC, pre-SMA and cerebellum. The subregion of the ACC demonstrating increased connectivity (BA 24/32) may support attention as well as pain/anti-nociceptive processing [21]. The pre-SMA supports motor planning [52], while the cerebellar simplex is related to cognitive processing [48] and is modulated by acupuncture [41] and pain [5]. Enhanced connectivity of these areas with the SMN may support linkage of lower order sensory/discriminative with higher-order affective/evaluative processing inherent to a complex sensory stimulus such as acupuncture.

Limitations

In the current study we evaluated the sustained effects of acupuncture on brain activity during rest following stimulation. Unfortunately, the delay which constitutes an optimal washout period for acupuncture's neurobiological effects remains unknown. To avoid contamination of the control conditions (SHAM), post-stimulus rest runs were separated by structural scanning, a minimum of 15 minutes. Furthermore, the “before” and “after” rest runs immediately preceded and followed active stimulation, respectively. Thus, our results reflect the direct influence of either ACUP or SHAM. Finally, the order of the ACUP and SHAM portions of the scan session was pseudo-randomized to avoid any order effects.

CONCLUSIONS

The current study evaluated acupuncture modulation of resting functional connectivity within the brain's DMN and SMN. Following verum acupuncture there was increased DMN connectivity with pain (ACC, PAG), affective (amygdala, ACC), and memory (hippocampal formation, MTG) related brain regions. Following acupuncture there was also increased SMN connectivity with pain related brain regions (ACC, cerebellum). We attributed differences between verum and sham acupuncture to more varied and stronger sensations evoked by verum acupuncture. Furthermore, increased DMN connectivity with the hippocampal formation, a region known to support memory and interconnected with autonomic brain regions, was anti-correlated with acupuncture-induced increase in a sympathetic related HRV metric (LFu), and correlated with a parasympathetic related HRV metric (HFu). Our results demonstrate for the first time that a complex somatosensory stimulation, acupuncture, can modulate the post-

stimulation spatial extent of resting state connectivity networks. Modulation of these networks and sympathovagal response to acupuncture may relate to acupuncture analgesia as well as other acupuncture associated therapeutic effects. Additionally, neuroimaging evaluation of chronic pain states has been notoriously difficult. Intrinsic functional connectivity, which we have demonstrated to be altered following our acute pain-like stimulus, may also be altered and/or dysfunctional in chronic pain patients – a hypothesis we plan to study in the future.

Acknowledgements

This research was supported by grants from NCCAM, NIH (P01-AT002048, K01-AT002166, F05-AT003770). We would like to thank Randy Buckner and Bruce Rosen for helpful comments during manuscript preparation. There are no conflicts of interest for any author.

Bibliography

1. Andersson S, Lundeberg T. Acupuncture - from empiricism to science: functional background to acupuncture effects in pain and disease. Medical Hypotheses 1995;45:271–281. [PubMed: 8569551]
2. Baliki, M.; Geha, P.; Apkarian, A.; Chialvo, D. Society for Neuroscience Annual Meeting. San Diego: 2007. Impaired brain de-activation in chronic pain..
3. Bantick SJ, Wise RG, Ploghaus A, Clare S, Smith SM, Tracey I. Imaging how attention modulates pain in humans using functional MRI. Brain 2002;125(Pt 2):310–9. [PubMed: 11844731]
4. Becerra L, Breiter HC, Wise R, Gonzalez RG, Borsook D. Reward circuitry activation by noxious thermal stimuli. Neuron 2001;32(5):927–46. [PubMed: 11738036]
5. Becerra LR, Breiter HC, Stojanovic M, Fishman S, Edwards A, Comite AR, Gonzalez RG, Borsook D. Human brain activation under controlled thermal stimulation and habituation to noxious heat: an fMRI study. Magn Reson Med 1999;41(5):1044–57. [PubMed: 10332889]
6. Beckmann CF, DeLuca M, Devlin JT, Smith SM. Investigations into resting-state connectivity using independent component analysis. Philos Trans R Soc Lond B Biol Sci 2005;360(1457):1001–13. [PubMed: 16087444]
7. Beckmann CF, Smith SM. Probabilistic independent component analysis for functional magnetic resonance imaging. IEEE Trans Med Imaging 2004;23(2):137–52. [PubMed: 14964560]
8. Berman BM, Lao L, Langenberg P, Lee WL, Gilpin AM, Hochberg MC. Effectiveness of acupuncture as adjunctive therapy in osteoarthritis of the knee: a randomized, controlled trial. Ann Intern Med 2004;141(12):901–10. [PubMed: 15611487]
9. Bingel U, Quante M, Knab R, Bromm B, Weiller C, Buchel C. Subcortical structures involved in pain processing: evidence from single-trial fMRI. Pain 2002;99(1−2):313–21. [PubMed: 12237210]
10. Birn RM, Diamond JB, Smith MA, Bandettini PA. Separating respiratory-variation-related fluctuations from neuronal-activity-related fluctuations in fMRI. Neuroimage 2006;31(4):1536–48. [PubMed: 16632379]
11. Biswal B, Yetkin FZ, Haughton VM, Hyde JS. Functional connectivity in the motor cortex of resting human brain using echo-planar MRI. Magn Reson Med 1995;34(4):537–41. [PubMed: 8524021]
12. Boly M, Balteau E, Schnakers C, Degueldre C, Moonen G, Luxen A, Phillips C, Peigneux P, Maquet P, Laureys S. Baseline brain activity fluctuations predict somatosensory perception in humans. Proc Natl Acad Sci U S A 2007;104(29):12187–92. [PubMed: 17616583]
13. Buchel C, Bornhovd K, Quante M, Glauche V, Bromm B, Weiller C. Dissociable neural responses related to pain intensity, stimulus intensity, and stimulus awareness within the anterior cingulate cortex: a parametric single-trial laser functional magnetic resonance imaging study. J Neurosci 2002;22(3):970–6. [PubMed: 11826125]
14. Buckner RL, Vincent JL. Unrest at rest: Default activity and spontaneous network correlations. Neuroimage. 2007
15. Castle M, Comoli E, Loewy AD. Autonomic brainstem nuclei are linked to the hippocampus. Neuroscience 2005;134(2):657–69. [PubMed: 15975727]
16. Chudler EH, Dong WK. The role of the basal ganglia in nociception and pain. Pain 1995;60(1):3–38. [PubMed: 7715939]

17. Clark KB, Naritoku DK, Smith DC, Browning RA, Jensen RA. Enhanced recognition memory following vagus nerve stimulation in human subjects. Nat Neurosci 1999;2(1):94–8. [PubMed: 10195186]
18. Craig AD. A new view of pain as a homeostatic emotion. Trends Neurosci 2003;26(6):303–7. [PubMed: 12798599]
19. Critchley HD, Mathias CJ, Josephs O, O'Doherty J, Zanini S, Dewar BK, Cipolotti L, Shallice T, Dolan RJ. Human cingulate cortex and autonomic control: converging neuroimaging and clinical evidence. Brain 2003;126(Pt 10):2139–52. [PubMed: 12821513]
20. Dale AM, Fischl B, Sereno MI. Cortical surface-based analysis. I. Segmentation and surface reconstruction. Neuroimage 1999;9(2):179–94. [PubMed: 9931268]
21. Davis KD, Taylor SJ, Crawley AP, Wood ML, Mikulis DJ. Functional MRI of pain- and attention-related activations in the human cingulate cortex. J Neurophysiol 1997;77(6):3370–80. [PubMed: 9212281]
22. De Luca M, Beckmann CF, De Stefano N, Matthews PM, Smith SM. fMRI resting state networks define distinct modes of long-distance interactions in the human brain. Neuroimage 2006;29(4): 1359–67. [PubMed: 16260155]
23. deCharms RC, Maeda F, Glover GH, Ludlow D, Pauly JM, Soneji D, Gabrieli JD, Mackey SC. Control over brain activation and pain learned by using real-time functional MRI. Proc Natl Acad Sci U S A 2005;102(51):18626–31. [PubMed: 16352728]
24. Derbyshire SW, Jones AK, Gyulai F, Clark S, Townsend D, Firestone LL. Pain processing during three levels of noxious stimulation produces differential patterns of central activity. Pain 1997;73(3): 431–45. [PubMed: 9469535]
25. Dhond RP, Kettner N, Napadow V. Do the neural correlates of acupuncture and placebo effects differ? Pain 2007;128(1−2):8–12. [PubMed: 17267130]
26. Dhond RP, Kettner N, Napadow V. Neuroimaging acupuncture effects in the human brain. J Altern Complement Med 2007;13(6):603–16. [PubMed: 17718643]
27. Faymonville ME, Roediger L, Del Fiore G, Delgueldre C, Phillips C, Lamy M, Luxen A, Maquet P, Laureys S. Increased cerebral functional connectivity underlying the antinociceptive effects of hypnosis. Brain Res Cogn Brain Res 2003;17(2):255–62. [PubMed: 12880897]
28. Fischl B, Sereno MI, Dale AM. Cortical surface-based analysis. II: Inflation, flattening, and a surface-based coordinate system. Neuroimage 1999;9(2):195–207. [PubMed: 9931269]
29. Flor H. Painful memories. Can we train chronic pain patients to 'forget' their pain? EMBO Rep 2002;3 (4):288–91. [PubMed: 11943751]
30. Fox MD, Raichle ME. Spontaneous fluctuations in brain activity observed with functional magnetic resonance imaging. Nat Rev Neurosci 2007;8(9):700–11. [PubMed: 17704812]
31. Fox MD, Snyder AZ, Vincent JL, Corbetta M, Van Essen DC, Raichle ME. The human brain is intrinsically organized into dynamic, anticorrelated functional networks. Proc Natl Acad Sci U S A 2005;102(27):9673–8. [PubMed: 15976020]
32. Fransson P. How default is the default mode of brain function? Further evidence from intrinsic BOLD signal fluctuations. Neuropsychologia 2006;44(14):2836–45. [PubMed: 16879844]
33. Goldberger AL, Amaral LA, Glass L, Hausdorff JM, Ivanov PC, Mark RG, Mietus JE, Moody GB, Peng CK, Stanley HE. PhysioBank, PhysioToolkit, and PhysioNet: components of a new research resource for complex physiologic signals. Circulation 2000;101(23):E215–20. [PubMed: 10851218]
34. Greicius MD, Flores BH, Menon V, Glover GH, Solvason HB, Kenna H, Reiss AL, Schatzberg AF. Resting-State Functional Connectivity in Major Depression: Abnormally Increased Contributions from Subgenual Cingulate Cortex and Thalamus. Biol Psychiatry. 2007
35. Greicius MD, Krasnow B, Reiss AL, Menon V. Functional connectivity in the resting brain: a network analysis of the default mode hypothesis. Proc Natl Acad Sci U S A 2003;100(1):253–8. [PubMed: 12506194]
36. Greicius MD, Srivastava G, Reiss AL, Menon V. Default-mode network activity distinguishes Alzheimer's disease from healthy aging: evidence from functional MRI. Proc Natl Acad Sci U S A 2004;101(13):4637–42. [PubMed: 15070770]

37. Guo ZL, Moazzami AR, Longhurst JC. Electroacupuncture induces c-Fos expression in the rostral ventrolateral medulla and periaqueductal gray in cats: relation to opioid containing neurons. Brain Res 2004;1030(1):103–15. [PubMed: 15567342]

38. Gusnard DA, Raichle ME. Searching for a baseline: functional imaging and the resting human brain. Nat Rev Neurosci 2001;2(10):685–94. [PubMed: 11584306]

39. Hammerschlag R, Zwickey H. Evidence-based complementary and alternative medicine: back to basics. J Altern Complement Med 2006;12(4):349–50. [PubMed: 16722781]

40. Han JS, Xie GX, Zhou ZF, Folkesson R, Terenius L. Acupuncture mechanisms in rabbits studied with microinjection of antibodies against beta-endorphin, enkephalin and substance P. Neuropharmacology 1984;23(1):1–5. [PubMed: 6201772]

41. Hui KK, Liu J, Marina O, Napadow V, Haselgrove C, Kwong KK, Kennedy DN, Makris N. The integrated response of the human cerebro-cerebellar and limbic systems to acupuncture stimulation at ST 36 as evidenced by fMRI. Neuroimage 2005;27(3):479–96. [PubMed: 16046146]

42. Janig W, Habler HJ. Sympathetic nervous system: contribution to chronic pain. Prog Brain Res 2000;129:451–68. [PubMed: 11098710]

43. Katz J, Melzack R. Pain 'memories' in phantom limbs: review and clinical observations. Pain 1990;43 (3):319–36. [PubMed: 2293143]

44. Kawakita K, Shinbara H, Imai K, Fukuda F, Yano T, Kuriyama K. How do acupuncture and moxibustion act? - Focusing on the progress in Japanese acupuncture research. J Pharmacol Sci 2006;100(5):443–59. [PubMed: 16799260]

45. Kong J, Gollub R, Huang T, Polich G, Napadow V, Hui K, Vangel M, Rosen B, Kaptchuk T. Acupuncture De Qi, from Qualitative History to Quantitative Measurement. Journal of Alternative and Complementary Medicine 2007;13(9)in press

46. Lowe MJ, Mock BJ, Sorenson JA. Functional connectivity in single and multislice echoplanar imaging using resting-state fluctuations. Neuroimage 1998;7(2):119–32. [PubMed: 9558644]

47. Mai, J.; Assheuer, J.; Paxinos, G. Atlas of the Human Brain. Elsevier Academic Press; San Diego: 2004.

48. Makris N, Hodge SM, Haselgrove C, Kennedy DN, Dale A, Fischl B, Rosen BR, Harris G, Caviness VS Jr. Schmahmann JD. Human cerebellum: surface-assisted cortical parcellation and volumetry with magnetic resonance imaging. J Cogn Neurosci 2003;15(4):584–99. [PubMed: 12803969]

49. Malik M, Camm A, members of the Task Force of the European Society of Cardiology. Heart rate variability: standards of measurement, physiological interpretation and clinical use. Circulation 1996;93(5):1043–65. [PubMed: 8598068]

50. Manheimer E, Linde K, Lao L, Bouter LM, Berman BM. Meta-analysis: acupuncture for osteoarthritis of the knee. Ann Intern Med 2007;146(12):868–77. [PubMed: 17577006]

51. McKiernan KA, Kaufman JN, Kucera-Thompson J, Binder JR. A parametric manipulation of factors affecting task-induced deactivation in functional neuroimaging. J Cogn Neurosci 2003;15(3):394–408. [PubMed: 12729491]

52. Nachev P, Wydell H, O'Neill K, Husain M, Kennard C. The role of the pre-supplementary motor area in the control of action. Neuroimage 2007;36(Suppl 2):T155–63. [PubMed: 17499162]

53. Napadow V, Kettner N, Liu J, Li M, Kwong KK, Vangel M, Makris N, Audette J, Hui KK. Hypothalamus and amygdala response to acupuncture stimuli in Carpal Tunnel Syndrome. Pain 2007;130(3):254–66. [PubMed: 17240066]

54. Napadow V, Makris N, Liu J, Kettner NW, Kwong KK, Hui KK. Effects of electroacupuncture versus manual acupuncture on the human brain as measured by fMRI. Hum Brain Mapp 2005;24(3):193–205. [PubMed: 15499576]

55. NIH. NIH Consensus Conference. Acupuncture. Jama 1998;280(17):1518–24. [PubMed: 9809733]

56. Ojemann JG, Akbudak E, Snyder AZ, McKinstry RC, Raichle ME, Conturo TE. Anatomic localization and quantitative analysis of gradient refocused echo-planar fMRI susceptibility artifacts. Neuroimage 1997;6(3):156–67. [PubMed: 9344820]

57. Oldfield RC. The assessment and analysis of handedness: the Edinburgh inventory. Neuropsychologia 1971;9(1):97–113. [PubMed: 5146491]

58. Price DD, Rafii A, Watkins LR, Buckingham B. A psychophysical analysis of acupuncture analgesia. Pain 1984;19(1):27–42. [PubMed: 6234501]

59. Seminowicz DA, Davis KD. Pain enhances functional connectivity of a brain network evoked by performance of a cognitive task. J Neurophysiol 2007;97(5):3651–9. [PubMed: 17314240]

60. Sparrow K. Analysis of heart rate variability in acupuncture practice: can it improve outcomes? Medical Acupuncture 2007;19(1):37–41.

61. Tjen ALSC, Li P, Longhurst JC. Midbrain vlPAG inhibits rVLM cardiovascular sympathoexcitatory responses during electroacupuncture. Am J Physiol Heart Circ Physiol 2006;290(6):H2543–53. [PubMed: 16428348]

62. Tsukayama H, Yamashita H, Kimura T, Otsuki K. Factors that influence the applicability of sham needle in acupuncture trials: two randomized, single-blind, crossover trials with acupuncture-experienced subjects. Clin J Pain 2006;22(4):346–9. [PubMed: 16691086]

63. Vincent CA, Richardson PH, Black JJ, Pither CE. The significance of needle placement site in acupuncture. J Psychosom Res 1989;33(4):489–96. [PubMed: 2795521]

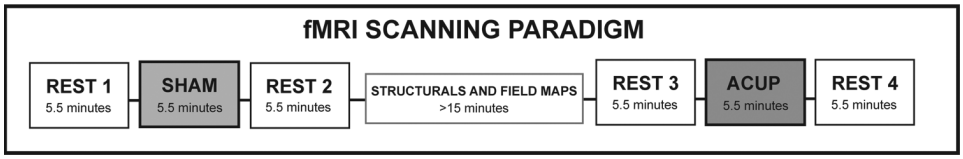

Figure 1. fMRI Scanning Paradigm

The order of SHAM and ACUP runs was pseudo-randomized across subjects and each was flanked by a 5.5 minute rest run. The SHAM and ACUP portions of the scan session were separated by structural and field map scans lasting no less than 15 minutes.

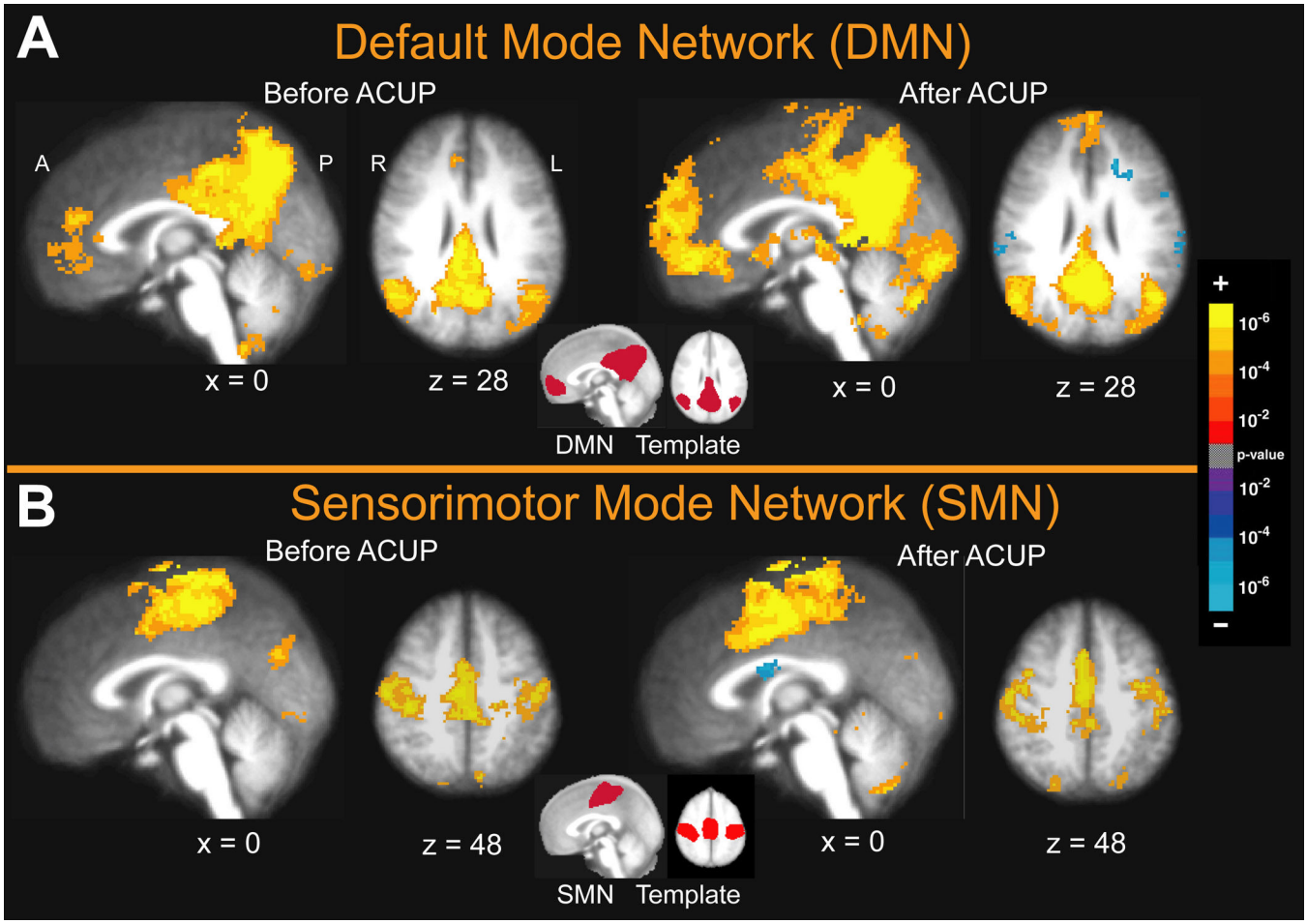

Figure 2. Group Maps for the Default Mode Network (DMN) and Sensorimotor Network (SMN), Before and After Acupuncture

The best-fit components were selected using template masks of the previously defined DMN and SMN shown in the center of each panel [6]. (A) The best fitting component for the DMN primarily involved the lateral parietal cortex, posterior cingulate, precuneus, and areas of the inferior, middle and superior frontal gyri. (B) The best fitting component for the SMN involved bilateral primary somatosensory and motor cortices, secondary somatosensory cortex and the supplementary motor area.

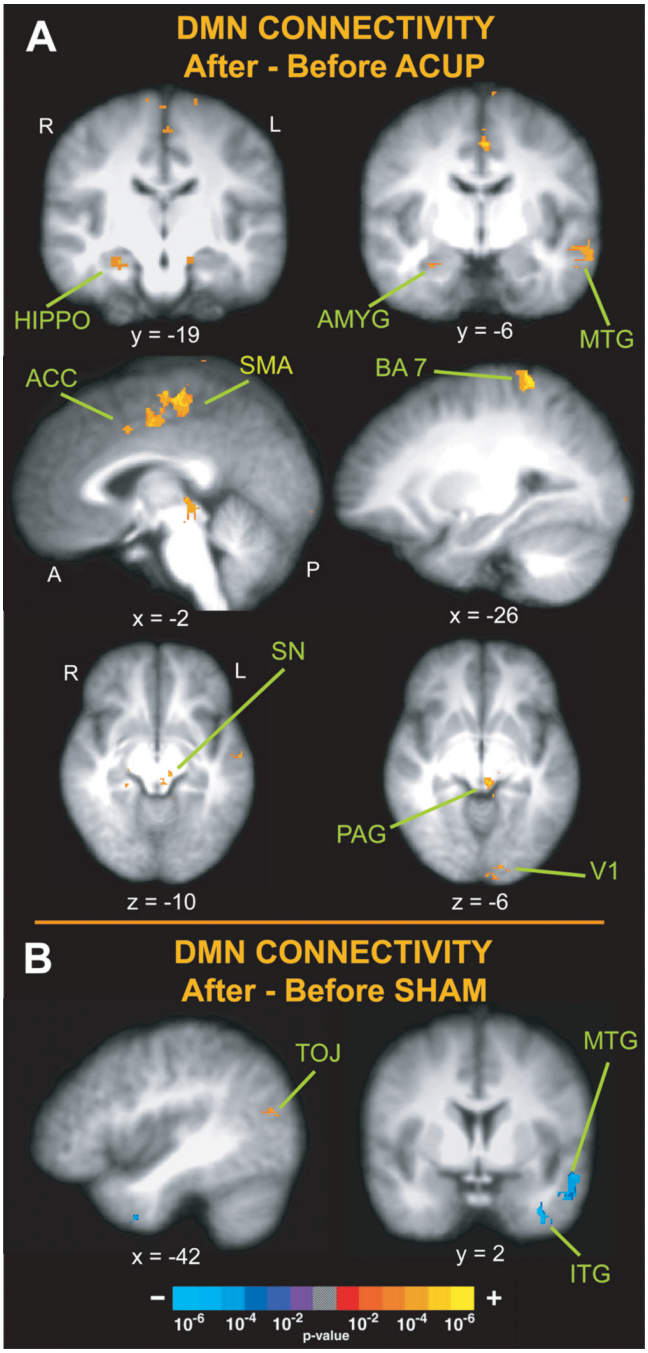

Figure 3. Changes in functional connectivity of the DMN following ACUP and SHAM (After – Before)

(A) Following verum acupuncture there was increased connectivity of the DMN with the amygdala (AMYG), hippocampal formation (HIPPO), middle temporal gyrus (MTG), anterior cingulate cortex (ACC), periaqueductal gray (PAG) and substantia nigra (SN) as well as posterior parietal (BA 7) and primary visual cortex (V1). **(B)** Following SHAM there was increased connectivity of the DMN with the temporo-occipital junction (TOJ) and decreased connectivity with the middle temporal and inferior temporal gyri (MTG, ITG).

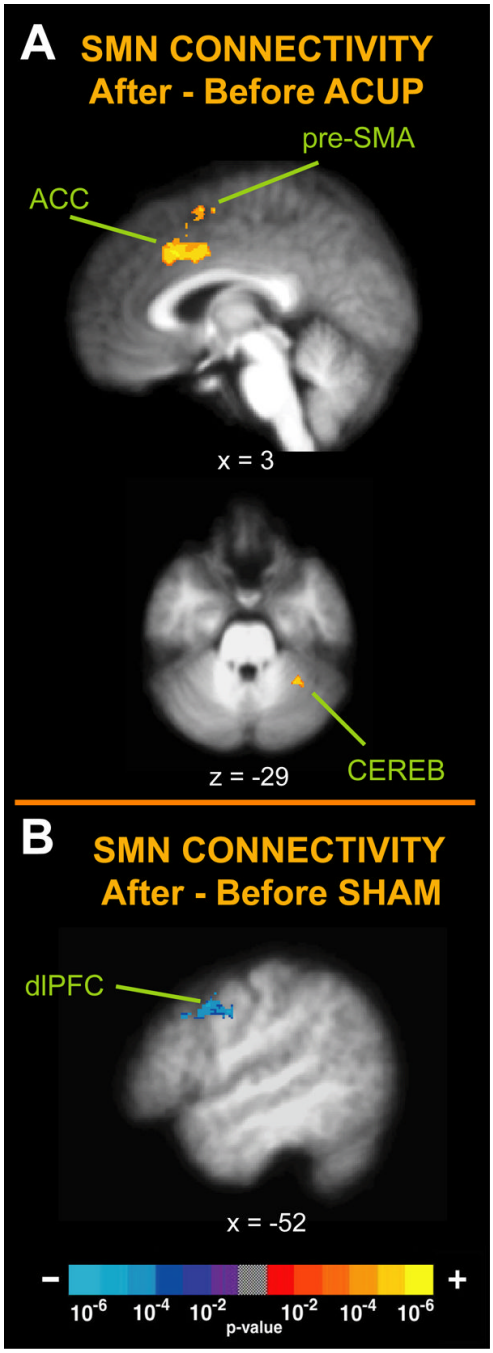

Figure 4. The changes in functional connectivity of the SMN for ACUP and SHAM (After – Before)
(A) Changes in the SMN for acupuncture involved increased connectivity with the ACC, pre-SMA, and the cerebellum (CEREB). **(B)** Following SHAM there was decreased connectivity for the SMN with the dorsolateral prefrontal cortex (dlPFC).

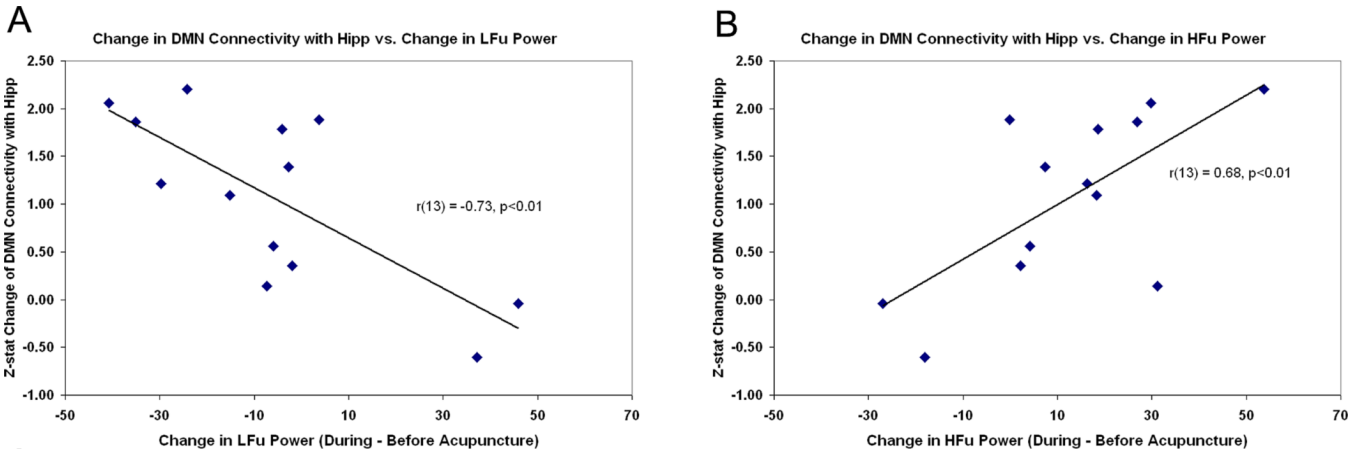

Figure 5. Changes in connectivity of the DMN following Acupuncture are correlated with HRV

Increased DMN-hippocampal connectivity post-acupuncture was negatively correlated with acupuncture-induced change in LFu (**A**), and positively correlated with HFu (**B**), suggesting that increased parasympathetic and decreased sympathetic modulation during ACUP is associated with increased post-stimulation DMN connectivity.

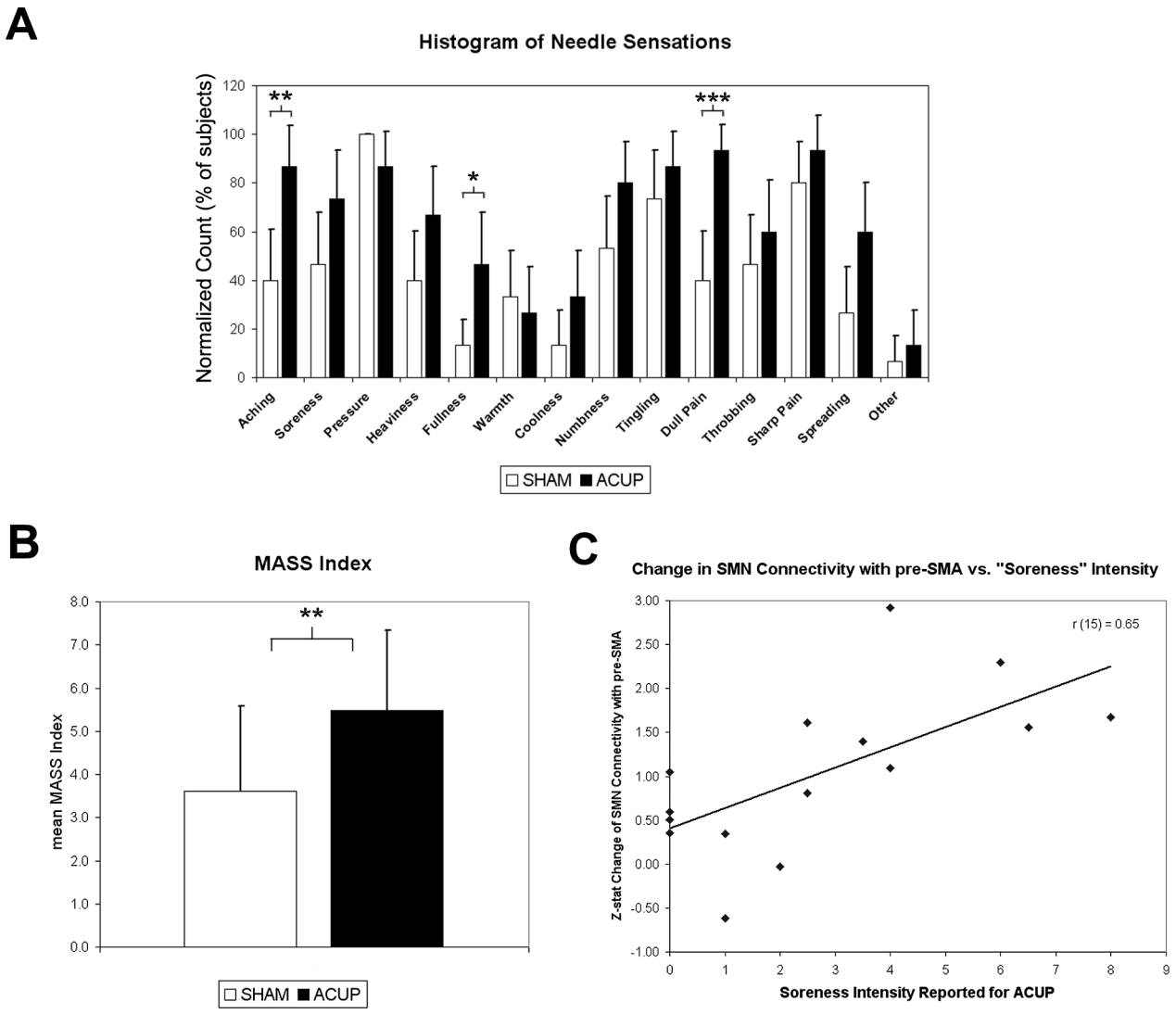

Figure 6. Results of psychophysical analysis

(A) Differences in the types of sensations elicited (expressed as a histogram) were found between ACUP and SHAM. ACUP more frequently induced “aching,” “fullness,” and “dull pain.” **(B)** MASS index, a measure of *deqi* intensity, was greater for ACUP compared to SHAM. (**C**) Results of a psychophysics/imaging correlation analysis: a trend was found for increasing ACUP evoked “soreness” correlating with increasing SMN connectivity with pre-SMA (r = 0.65, p=0.081, Bonferroni corrected), a result consistent with the hypothesis that changes in resting SMN connectivity are related to the sensations evoked by acupuncture stimulation. n.b. Error bars in **A** represent a 90% confidence interval for binomial distribution. Sensations on the abscissa are in the order presented to the subjects. Error bars in **B** represent standard deviation. *p<0.05, **p<0.01, ***p<0.005.

Table 1

Brain regions in the DMN and SMN modulated by both verum and sham acupuncture.

	Hemisphere	BA	Z-score	x	y	z	Average Z-score Before	Average Z-score After
DMN: ACUP								
Amygdala	Right		2.45	30	−7	−23	0.54	3.2
Hippocampal formation	Right		3.39	27	−17	−19	1.51	4.27
Periaqueductal Grey	Left		3.44	−3	−30	−6	0.49	3.61
Substantia Nigra	Left		3.30	−9	−26	−12	0.72	3.94
Middle Temporal Gyrus	Left	21	3.96	−57	3	−24	0.75	3.81
Supplementary Motor Area	Left	6	4.12	−1	−21	59	−0.13	3.31
Anterior Cingulate Cortex	Left	24	3.03	−4	8	41	0.21	3.23
Posterior Parietal Cortex	Left	7	4.77	−24	−43	70	−1.11	3.31
Visual Cortex	Left	17	3.55	−7	−93	−2	0.85	3.52
DMN: SHAM								
Temporal Occipital Junction	Left	37/19/39	2.94	−45	−83	11	0.00	3.06
Middle Temporal Gyrus	Left	21	−3.55	−54	3	−17	3.98	1.98
Inferior Temporal Gyrus	Left	20	−4.16	−34	5	−41	3.74	0.78
SMN: ACUP								
Anterior Cingulate Cortex	Right	24/32	4.22	5	21	38	0.78	3.53
Pre-SMA	Right	8/6	4.00	7	6	59	1.26	4.15
Cerebellum, VI /	Left		3.59	−32	−49	−31	−0.10	3.21
SMN: SHAM								
Dorsolateral Prefrontal Cortex	Left	8	−3.37	−52	9	39	3.54	1.25